Flow Control with Ruler Electromagnetic Braking (EMBr) in Continuous Casting of Steel Slabs

THOMAS, Brian G..; SINGH, Ramnik; CHAUDHARY, Rajneesh; and VANKA, Pratap
Department of Mechanical Science & Engineering, University of Illinois at Urbana-Champaign
1206 West Green Street, Urbana, IL, USA, 61801; bgthomas@illinois.edu

Abstract: Electromagnetic forces are an important tool to control fluid flow in the mold, combined with other casting conditions, nozzle, and mold geometry. Methods include static magnetic fields (local and ruler EMBr), and time-varying magnetic fields, such as electromagnetic stirring, (EMS), multi-mode EMS, electromagnetic level stabilizers (EMLS), and electromagnetic level accelerators (EMLA). Optimal use can stabilize flow, leading to fewer surface defects, fewer inclusions, and improved microstructure. Numerical models are an important tool to optimize electromagnetic flow control, but the complexities make validation essential. This paper presents transient flow predictions using high-resolution computational models, validated with analytical solutions, laboratory measurements, and plant measurements. The results provide new insights into the optimal position of EMBr fields. Locating the field below the nozzle ports leads to stable, higher-velocity surface flow.

Key words: EMBr**;** Large Eddy Simulation; computational model; transient, unstable flow

1 Introduction

Steel quality depends greatly on the turbulent flow in the mold during continuous casting. Surface defects due to meniscus freezing arise if the surface flow near the slab-metal interface is too slow to prevent hook formation and to provide convective mixing to help melt the mold powder. Slag entrainment, and surface defects from level fluctuations will occur if the surface flow is too fast, or the liquid profile is not flat enough.[1-2] Finally, and most importantly, intermittent defects of many kinds may occur due to excessive transient fluctuations in the liquid level.

Flow in the mold region is controlled by the nozzle and mold geometry, casting speed, nozzle submergence depth, argon gas injection, and the application of electromagnetic forces.[1] Electromagnetic forces are optionally applied as either static or moving magnetic fields through the thickness of the strand. Static (DC) electromagnetic fields induce current in the conducting liquid steel, which in turn, generates forces which directly oppose the flow, so are they referred to as “brakes”, or “EMBr”.[3] As shown in Fig. 1, EMBr fields include local cylindrical-shaped fields, wide “ruler-shaped” magnetic fields across the entire mold width, and double-ruler fields, sometimes referred to as Flow-Control, or “FC-mold” fields.[4]

Moving (AC) fields originated with electromagnetic stirring (EMS), where phase-shifting the fields from several series of magnetics to make the net field move in opposite directions on opposite sides of the strand induces rotating flow, usually in the transverse plane in the mold (Mold-EMS)[5-6] or electromagnetic rotary stirring (EMRS.[7-8] Making the fields move in the same direction, sometimes called “multi-mode EMS”, can induce accelerating flow, electromagnetic level accelerator (EMLA), or decelerating flow, electromagnetic level stabilizer (EMLS).[7-8]

Electromagnetic forces offer an advantage over other flow-control parameters because the induced force varies with the strength of the liquid metal flow, giving the system the theoretical ability to be self-stabilizing for turbulent flow variations. In practice, this is difficult to achieve.

This work investigates the effect of EMBr ruler-shaped magnetic fields on transient turbulent flow in the continuous casting nozzle and mold using Large-Eddy-Simulation (LES) models. The model is first rigorously validated with velocity measurements in a small scale GaInSn model using ultrasonic Doppler velocimetry (UDV) before using it to investigate the effect of electromagnetic braking on the turbulent flow behavior. Practical insights are revealed about the effect of the location of ruler brakes in stabilizing the turbulent flow to lessen associated defects in the continuous casting process.

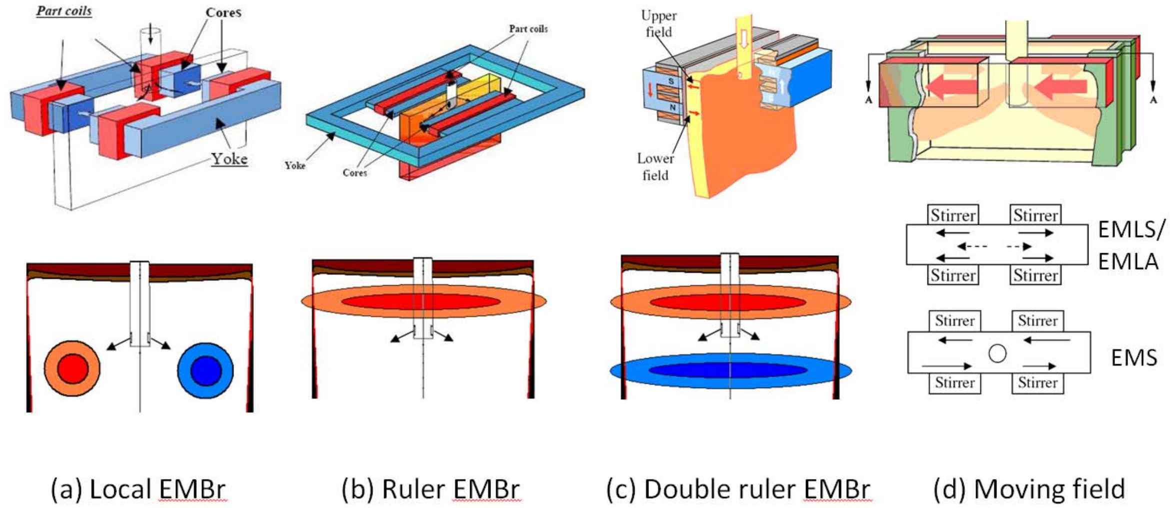

Fig.1 Types of electromagnetic flow control systems in slab casting showing magnet configuration (top) and magnetic field location (bottom)

2 Caster Geometry and Measurements

The current work investigates turbulent flow in a small-scale liquid metal GaInSn physical model of the continuous steel-slab casting process at Forschungszentrum Dresden-Rossendorf (FZD), Dresden, Germany where velocity measurements have been performed in previous works,[9-11] including the effects of EMBr.[9-10] Further details on the physical GaInSn model and the measurements can be found in Timmel et al.[9-11] and in Chaudhary et al.[12]

An ultrasonic velocity profiler was used to measure instantaneous horizontal velocity histories at various vertical positions across the midplane along different horizontal lines. The GaInSn model of the mold region has 140 mm (width) x 35 mm (thickness) x 300 mm (height) and vertical walls. The model features a 300-mm long cylindrical inlet nozzle with 10 mm inner bore diameter, a well-shaped bottom and zero-degree (horizontal) angled bifurcated ports with port-to-bore ratio of 3.31. Figure 2 shows schematics of this facility with front-, side- and bottom-views.

The “orange” rectangle in the front view of Fig. 2 shows where the magnetic coil for the single-ruler brake is located, with the maximum field strength at 92-mm below the top free surface of the liquid. The exact shape of the magnetic field is plotted in Fig. 3, which shows almost constant strength except in the vertical direction. Table I contains geometric details, casting conditions, physical properties of GaInSn, and the EMBr conditions for this study.[12-14] A scaling factor of six over the GaInSn model gives mold dimensions typical of a commercial continuous slab caster.

Four simulation cases are presented here: 1) no EMBr, 2) with ruler EMBr positioned over the nozzle (92-mm below the top surface of the scale-physical model with insulated walls), 3) with ruler EMBr positioned below the nozzle (121-mm below mold top and insulated), and 4) Case 2 with conducting solid-shell walls like the real caster.

3 Computational Model

The in-house Large Eddy Simulation code, CUFLOW, used in this work employs a finite volume discretization on a structured Cartesian grid to solve the coupled Navier-Stokes and Magneto-Hydro-Dynamic (MHD) equations.[12-13] A geometric multigrid solver is used to solve the pressure Poisson equation (PPE) and electric Poisson equation (EPE). The model code was implemented on a NVIDIA C2075 GPU graphics processing unit (GPU), which greatly lowered computation time.[13] The flow domain, shown in Fig. 4, includes only the liquid. The GaInSn mesh had 7.6 million brick cells and took 10 days to simulate 27s.

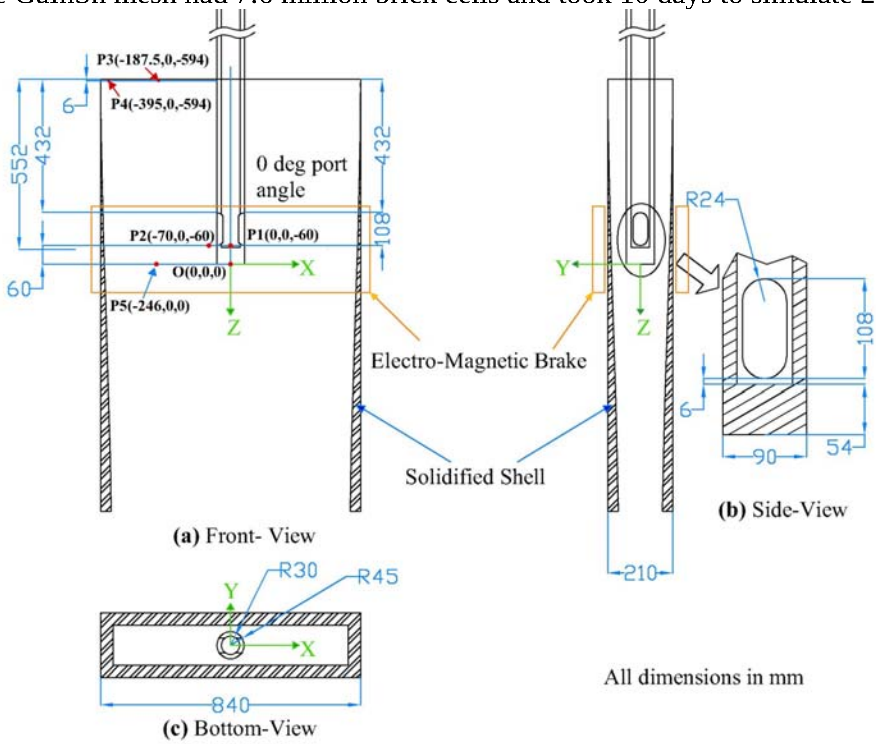

Fig.2 Geometry of the real caster with a rectangle showing the ruler EMBr location.

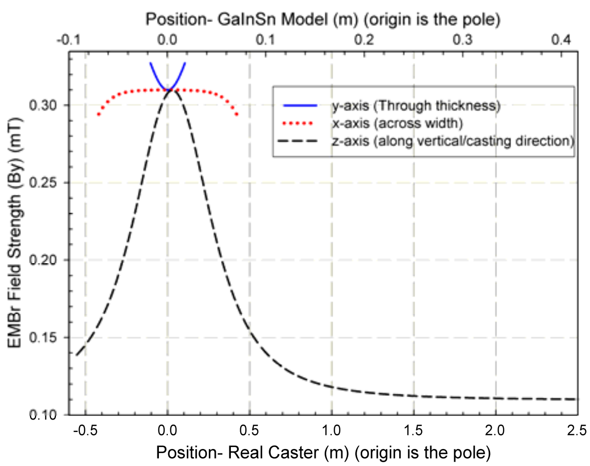

Fig. 3 Applied magnetic field in the x,y and z directions for GaInSn model and real caster.

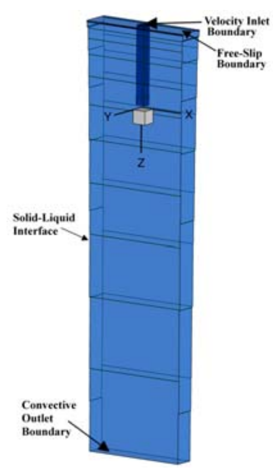

Fig. 4 Isometric view of computational flow domain (real caster).

The nozzles were very long, (20 diameters), so that the inlet flow control conditions had no effect. This was modeled by truncating the nozzles at the level of the liquid surface and an inlet mapping condition was applied to achieve fully developed pipe flow. The top free surface in the mold was a free-slip boundary with zero normal velocity and zero normal derivatives of tangential velocity. Convective boundary conditions were applied for all three velocity components at the two mold outlet ducts on the narrow faces (NF) in the scaled model and across the open bottom of the real caster domain. All other boundaries were solid walls and Werner-Wengle wall treatment was applied. In the real caster the boundaries, between the shell and fluid region, were initialized with fixed downward vertical velocity equal to the casting speed, which accounts for solidification as mass transfers from the fluid region to the solidified shell. The No-EMBr cases were started with zero initial velocity and the EMBr cases were started from the fully-developed No-EMBr flowfield. The fluid flow equations were solved only in the fluid-flow domain but the MHD equations were solved in the entire computational domain, including the brass walls for the GaInSn domain and the shell (shaded) region for the real caster domain.

Table 1 Casting Geometry and Process Parameters

	GaInSn Model	**Real Caster**
Volume flow rate | inlet velocity	110 mL/s | 1.4 m/s	4.8 L/s | 1.7 m/s
Casting speed	1.35 m/min	1.64 m/min
Mold width (=Domain width)	140 mm	840 mm
Mold thickness (=Domain thickness)	35 mm	210 mm
Mold length	330 mm	1980mm
Domain length	330 mm	3200 mm
Nozzle port (width x height)	8 mm x 18 mm	48 mm x 108 mm
Nozzle bore diameter (inner/outer)	10 mm/ 15 mm	60 mm / 90 mm
SEN submergence depth	72 mm	432 mm
Shell thickness	Wide faces only - 0.5 mm	s(mm)= $k\sqrt{t(s)}$;
Wall material	Brass	Solidified steel
Fluid material	GaInSn eutectic alloy	Molten steel
Viscosity	0.34 x 10^{-6} m^2/s	0.86 x 10^{-6} m^2/s
Fluid density	6360 Kg/m^3	7000 Kg/m^3
Conductivity of liquid (σ_{liquid})	3.2 x 10^6 /Ωm	0.714 x 10^6 /Ωm
Conductivity of walls (σ_{wall})	15 x 10^6 /Ωm	0.787 x10^6 /Ωm
Conductivity ratio(c_w)	0.130	0.130
Nozzle port angle	0 deg	0 deg
Gas injection	No	No
Reynolds number Re, from nozzle diameter	41,176	118,604
Froude number (Fr, based on mold width)	1.19	0.59
Stuart number (N, based on mold width)	4.84	4.84

4 Computational Model Validation

Time-averaged horizontal velocity contours from LES-CU-FLOW are compared in Fig. 5 with UDV measurements at the mold-mid plane for the first three cases.[11] The LES predictions match well with no EMBr and for both single-ruler EMBr cases. As documented in previous work[12] and also stated by Timmel et al.,[9-11] the measurements close to the SEN and close to narrow face are inaccurate, likely due to interaction effects near walls, and spatial resolution. Note that each jet appears to have two high-velocity peak spots. This is an artifact of the post-processing method, which interpolates only 10 lines of measured data. The calculated case with EMBr uses the same post-processing method, and produces the same two peaks. Actually, the jet is continuous, as shown with high-resolution post-processing in the other 2 frames.

A comparison of the model predictions with measurements of transient horizontal velocities at a typical point in the jet in the mold midplane is presented in Fig. 6 for 12 sec of data. As previously shown in,[12] the measurements have ~0.2s temporal filtering so are unable to capture the higher frequencies. This measurement limitation can be seen clearly in Fig. 6.

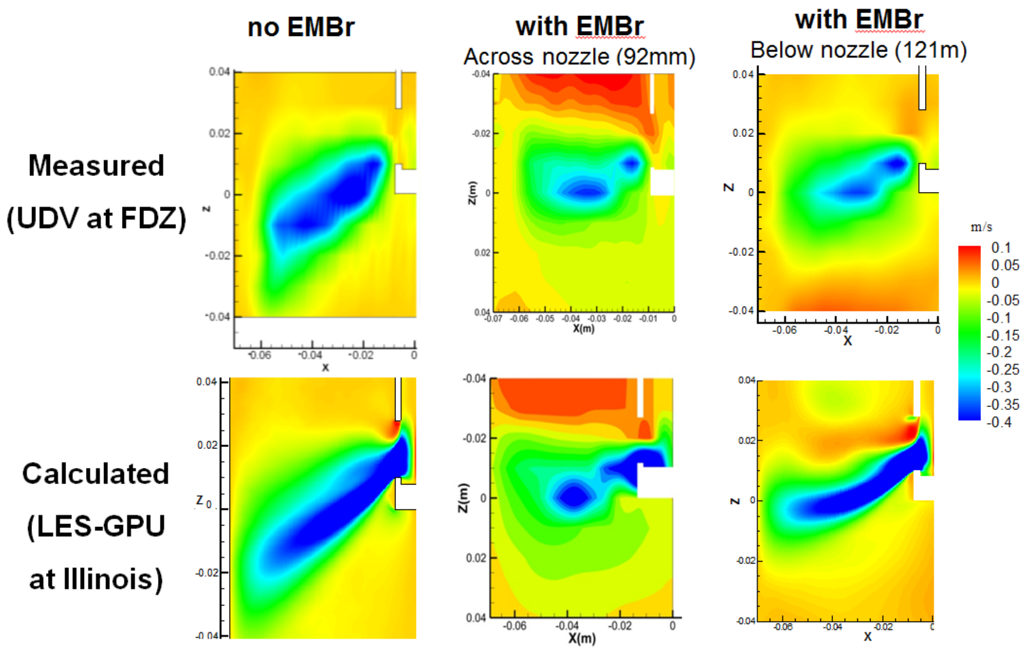

Fig. 5 Comparison of measured and simulated UDV signals

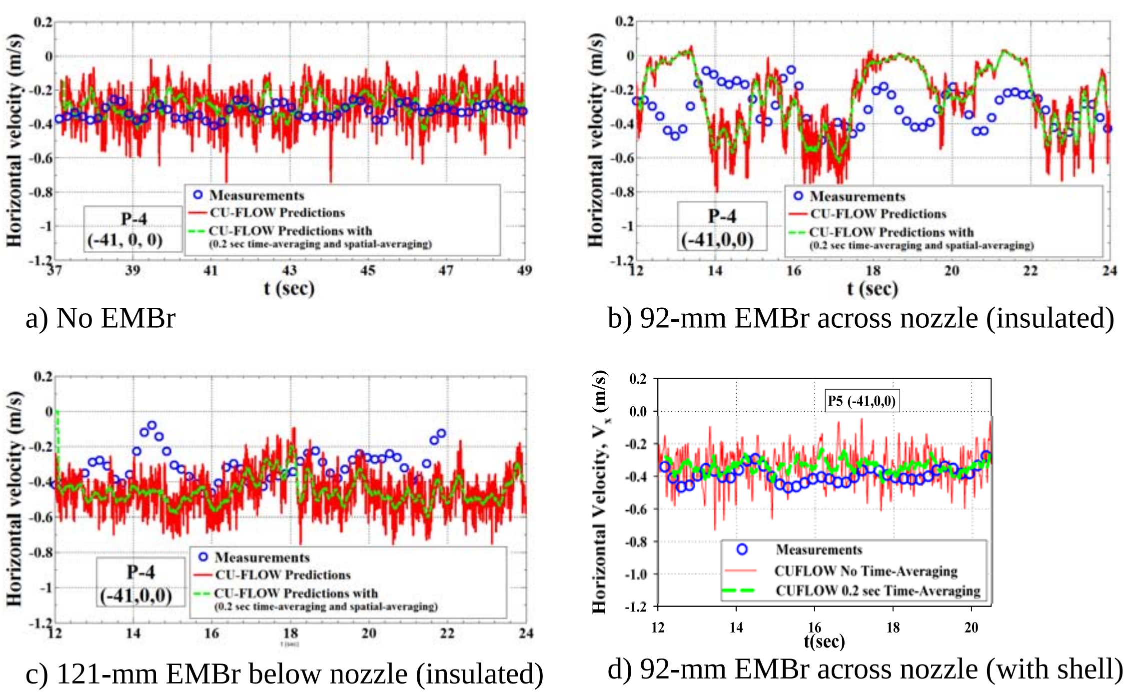

a) No EMBr

b) 92-mm EMBr across nozzle (insulated)

c) 121-mm EMBr below nozzle (insulated)

d) 92-mm EMBr across nozzle (with shell)

Fig. 6 Typical transient horizontal velocity, comparing predictions and measurements.

Applying 0.2 sec moving time-average and appropriate spatial averaging to the predictions enables them to match well with the variations in the measured signals. Spatial averaging alone was found to have negligible effect.[12] Very large, low-frequency variations are observed in each of the predicted and measured signals, especially for the 92-mm EMBr case with insulated walls. Including the conducting steel shell (or a metal plate to represent it in the physical model) greatly increases flow stability for all cases with EMBr.

5 Results

Having validated the LES model, its predictions of velocity, turbulence, and flow structures in the mold were evaluated for the four cases. The effects of electromagnetic braking on both the time-averaged and instantaneous flow structures in the liquid-metal caster model are investigated and presented in Fig. 7, based on ~49 sec of simulation results for non-EMBr and ~33 sec of simulation results for EMBr cases (starting with no-EMBr results at 49 sec).

5.1 Flow Pattern

With the EMBr ruler brake positioned directly over the nozzle ports, (92-mm case with insulated walls) the jet shows strong right-left asymmetry in the time-average flow field even after 28s. In fact, over 200s was required to achieve symmetrical flow pattern, which was only possible with a coarser mesh. This behavior is due to the long-term, large-scale, low-frequency transient flow structures that develop for this case. It arises because the strong magnetic field positioned directly across the nozzle bottom magnifies small differences in the low-frequency variations of the two jets exiting the ports: where they deflect either upwards or downwards and persist into the mold to form long-lasting, large-scale flow structures. The jets in this case form a tight upper roll on one side while hitting the narrow face wall on the other side, to send flow straight upward and downward. The slight asymmetry in the magnetic field (See Fig. 3, width direction) was ruled out from being responsible for the huge flow variations by performing a ~48sec simulation with a perfectly-symmetric magnetic field, and again observing unstable asymmetric flow.

With the lower 121-mm EMBr (insulated) ruler case, the weaker magnetic field in the nozzle bottom makes flow relatively more turbulent in the nozzle. The jets retain their turbulence across a wide frequency range. The jets then exit the ports with a shallower downward angle. They are further deflected upward by the EMBr field and consistently impinge almost horizontally onto the narrow faces, sending strong upward flows towards the top surface, and a classic double-roll flow pattern. This produces the fastest surface velocity of all the cases.

With a conducting metal shell wall, the flow pattern becomes much more stable. This is because the current can make its way through the solid, stationary metal walls without inducing new flows which are very sensitive to the current path. Although only the 92-mm case is presented, the shell walls greatly stabilized the flow for all cases studied, including the 121-mm case.

Modeling the full scale steel caster gives flow patterns which are qualitatively similar to the flows simulated in the $1/6^{th}$ physical model.[14] In order to give quantitative velocity predictions, however, it is necessary to satisfy scaling criteria involving Froude number.[14]

5.2 Surface Velocity

The horizontal “surface” velocity below the top free surface is presented in Fig. 8. As explained previously, surface flow is of great practical importance to the commercial continuous-casting process. The GaInSn physical model and corresponding real caster has a very deep submergence relative to a typical caster so tends to have much slower surface flows.

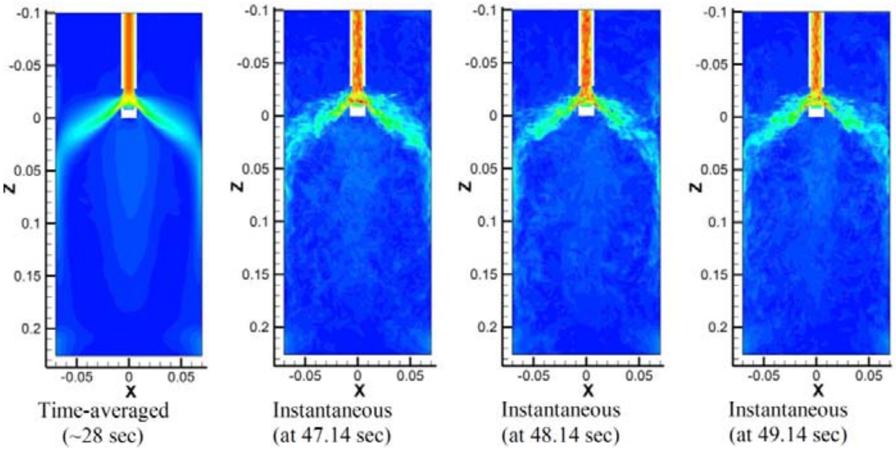

a) No EMBr

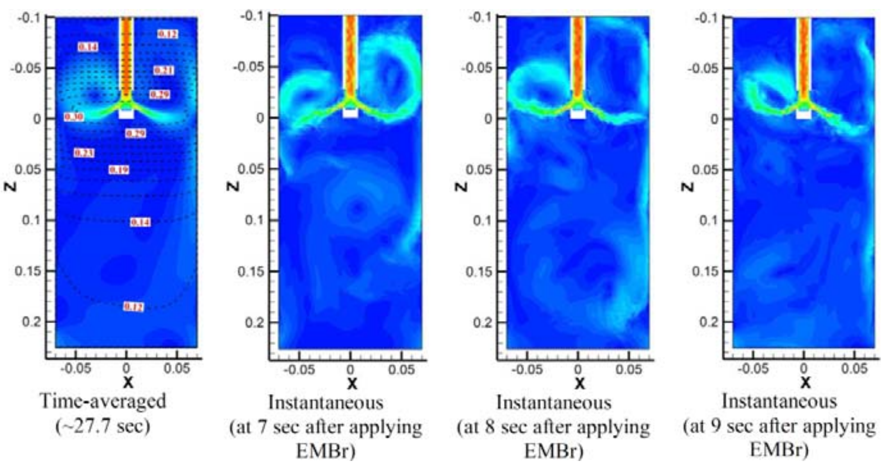

b) With EMBr across nozzle (92-mm insulated case)

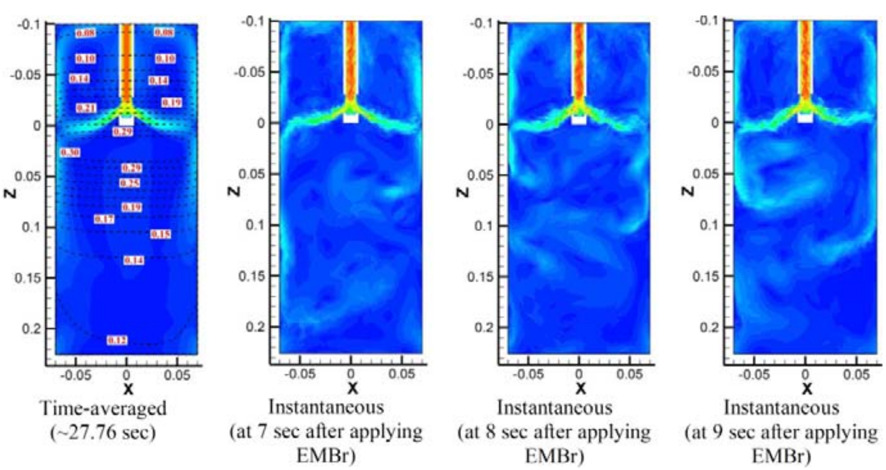

c) With EMBr below nozzle (121-mm insulated case)

Fig. 7 Velocity magnitude contours: time-averged (left) and transient (3 right frames)

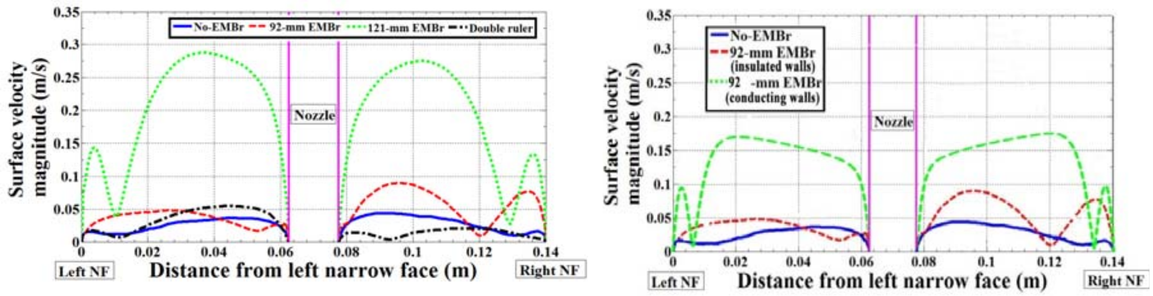

Fig. 8 Horizontal velocity profiles across top surface

The no-EMBr case would thus likely be prone to meniscus freezing and related defects. Applying the 121-mm EMBr increases surface velocity significantly and stably, and thus could act as an effective non-intrusive, easily-adjustable method to increase free surface velocity as needed to reduce meniscus freezing defects. The 92-mm EMBr configuration produces surface velocity between the no-EMBr and 121-mm EMBr cases. The upward flow velocity along the narrow face near the free surface controls the surface flow.

5.3 Surface Turbulent Kinetic Energy

The turbulent kinetic energy (TKE) at the top free surface is important to steel quality and is presented in Fig. 9. The no-EMBr case shows low TKE, and appears to have insufficient surface mixing to prevent meniscus freeing defects. The flow produced with the EMBr ruler positioned directly over the ports (92-mm EMBr case) experiences the highest TKE almost everywhere. The high turbulence levels and large right-left asymmetries with this ruler indicate detrimental unstable flow with very long time periods, and also making the averaging time of 28s insufficient.

The TKE with the 121-mm EMBr is expected to be stronger than without EMBr, owing to the higher surface velocity for this case. Moreover, this ruler maintains reasonable stability, as shown by symmetric turbulence on both sides of the mold surface. Thus, this ruler location produces the best flow to prevent surface defects, as previously discussed.

Adding metal walls to simulate the conducting steel shell greatly stabilizes the flow field, for every case (only the 92-mm case is shown here). This decreases the surface turbulence TKE, as shown in Fig. 9 for the 92-mm case.

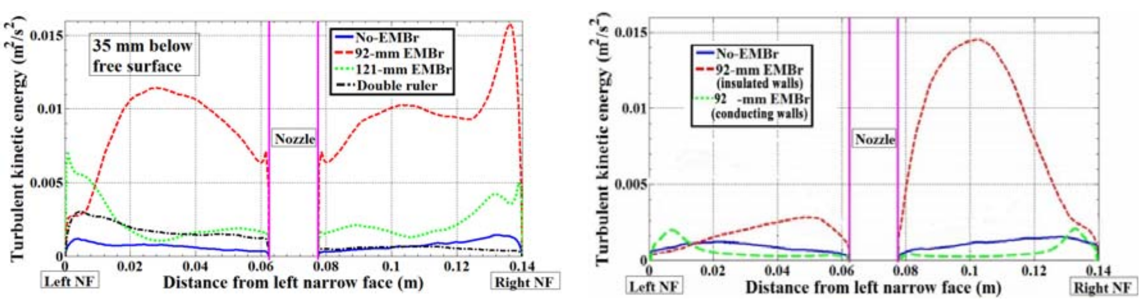

Fig. 9 Kinetic energy profiles across top surface

6. Conclusions

The current work investigates the effect of electromagnetic braking (EMBr) on turbulent flow during continuous casting of steel slabs with deep nozzle submergence using transient Large Eddy Simulations. The computations reasonably match both time-average and filtered transient histories of Ultrasonic Doppler Velocimetry measurements in a small scale GaInSn model of the studied geometry, including a no-EMBr case, and two single-ruler EMBr cases [18]. The model also captures high-frequency velocity fluctuations, and velocities near the SEN and NF, which are missed by the measurements. Model applications reveal the following insights regarding electromagnetic braking effects on transient flow:

• Applying a magnetic field at or below the nozzle deflects the jet upward, leading to a shallower downward jet angle and higher surface velocity for the time-averaged flow.

• The jet tends to deflect away from the region of the strongest magnetic field. Thus, applying the strongest magnetic field directly across the nozzle ports suppresses high-frequency turbulence in the jet, and leads to unstable large-scale, low-frequency time-varying vortical structures in the x-z plane of the upper and lower recirculation regions in the mold. This practice is generally detrimental to steel quality so should be avoided.

• Moving the maximum magnetic field below nozzle bottom allows the jet to retain its turbulence in a wide range of frequencies. This tends to deflect the jet consistently upward, leading to more stable flow in the mold. For a deep nozzle submergence, this practice increases surface flow and mixing to lessen quality problems related to meniscus freezing.

• With insulated walls (no steel shell), the flow is much more stable than without EMBr. In a real steel caster, the steel shell conducts current which stabilizes the flow with EMBr. Flow in the real steel caster matches closely with that in the physical model with conducting metal walls attached to the plastic container. Thus, static magnetic fields can deflect the liquid steel jets to either increase or decrease surface velocity and turbulence, depending on the position of the maximum field strength relative to the jets exiting the nozzle. This gives EMBr the potential to control flow-related defects if optimized.

7 References

[1] B. G. Thomas, B.G., “Fluid flow in the mold,” Chapter 14 in Making, Shaping and Treating of Steel, 11th Edition, v. 5, Casting Volume, Editor: A. Cramb, AISE Steel Foundation, Oct. 2003, Pittsburgh, PA, pp. 14.1-14.41.

[2] Hibbeler, L.C., and Brian G. Thomas, “Mold Slag Entrainment Mechanisms in Continuous Casting Molds”, AISTech 2013 Proceedings, Pittsburgh, PA, May 6-8, 2013, Assoc. Iron Steel Technology, Warrendale, PA, pp. 1215-1230.

[3] B. G. Thomas, and L. Zhang, "Review: Mathematical Modeling of Fluid Flow in Continuous Casting of Steel", ISIJ International, 2001, Vol. 41, No. 10, pp. 1181-1193.

[4] K. Cukierski and B. G. Thomas, “Flow Control with Local Electromagnetic Braking in Continuous Casting of Steel Slabs,” Metall. Mat. Trans. B, 39, 1, 2008, 2007, pp. 94-107.

[5] H.R. Hackl, A.F. Lehman, J.E.A. Eriksson, and S.G. Kollberg: AISTech Preliminary Program, AIST, Warrendale, PA, 2006.

[6] J. Nakashima, J.A. Kiyose, Y. Ohtani, J. Fukuda, T. Kawase, and M. Doki: Nippon Steel Technical Report No. 86, Nippon Steel, 2002, No. 86, pp. 61–67.

[7] P.H. Dauby and S. Kunstreich: Ironmaking and Steelmaking, 2005, vol. 32 (1), pp. 80–86.

[8] K. Okazawa, T. Takehito, J. Fukuda, T. Kawase, and M. Toki: ISIJ Int., 2001, vol. 41 (8), pp. 851–58.

[9] K. Timmel, S. Eckert, and G. Gerbeth, Experimental investigation of the flow in a continuous-casting mold under the influence of a transverse, direct current magnetic field, Metall. Mat. Trans. B, 2011, vol. 42, 1, pp. 68-80.

[10] K. Timmel, X. Miao, S. Eckert, D. Lucas, and G. Gerbeth, Experimental and numerical modeling of the steel flow in a continuous casting mould under the influence of a transverse DC magnetic field, Magnetohydrodynamics, 2010, vol. 46, 4, pp. 337-448.

[11] K. Timmel, S. Eckert, G. Gerbeth, F. Stefani, and T. Wondrak, Experimental modeling of the continuous casting process of steel using low melting point alloys – the LIMMCAST program, ISIJ International, 2010, 50, No. 8, pp. 1134-1141.

[12] Chaudhary, Rajneesh, Surya P. Vanka, and Brian G. Thomas, “Transient Turbulent Flow in a Liquid-Metal Model of Continuous Casting, Including Comparison of Six Different Methods”, Metallurgical and Materials Trans. B, 42B: 5, 987-1007, 2011.
[13] Chaudhary, R., B.G. Thomas, and S.P. Vanka, “Effect of Electromagnetic Ruler Braking (EMBr) on Transient Turbulent Flow in Continuous Slab Casting using Large Eddy Simulations,” Metall. Mat. Trans. B, 43B:3, 532-553, 2012
[14] Singh, R., B.G. Thomas, and P. Vanka, “Effects of a Magnetic Field on Turbulent Flow in the Mold Region of a Steel Caster,” Metall. Mat. Trans. B, in press, May, 2013.

8 Acknowledgements

This work was supported by the National Science Foundation Grant CMMI 11-30882 and the Continuous Casting Consortium. The authors are also grateful to K. Timmel, S. Eckert and G. Gerbeth from the MHD department, Forschungszentrum Dresden-Rossendorf (FZD), Dresden, Germany for providing the velocity measurement database of the GaInSn model experiment.